PAPER

Check for updates

Design and catalytic application of Zr based metal–organic framework with pillared layer mixed ligands for the synthesis of pyrazolo[3,4-b]pyridine derivatives *via* a cooperative vinylogous anomeric-based oxidation

Hossein Ahmadi,[a] Mohammad Ali Zolfigol, [iD] *[a] Maryam Hajjami, [iD] *[a] Mahmoud Zarei, [iD] *[b] Mojtaba Hosseinifard [iD] [c] and Yanlong Gu [iD] [d]

The post-synthesis of metal–organic frameworks (MOFs) plays a valuable role in enhancing their properties and functionalities. Herein a pillared layer mixed ligand metal–organic framework, derived (DMOFs) from 2-aminoterephthalic acid (BDC-NH₂) as an *O*-donor and 1,4-diazabicyclo[2.2.2]octane (DABCO) as a *N*-donor linker based on Zr as a metal, which is functionalized with Cu(OAc)₂ as a high-efficiency heterogonous catalyst for the synthesis of pyrazolo[3,4-b]pyridine derivatives. This presented work emphasizes the importance of the designability of an MOF and its multiple applications in organic chemistry, especially the synthesis of biologically active candidate compounds while considering the green chemistry principles.

Introduction

In recent decades, the design, synthesis and applications of porous catalyst such as metal–organic frameworks (MOFs) have been a major subject of research. This class of crystalline hybrid materials, composed of metal centers and various organic ligands, offers unique chemical versatility, a customizable framework, and exceptionally large and permanent internal porosity.[1–6] The MOFs possess a high surface area, significant porosity, and the ability to chemically adjust through the modification of organic ligands, enhancing their efficacy as adsorbents, gas separation, catalysts, drug delivery and energy storage. The selection of an appropriate synthetic route plays a crucial role in designing MOFs with specific sizes, morphologies, and nanostructures. This necessity has spurred the development of new methods over the years. Recent advancements in MOF nanostructures have been propelled by the introduction of innovative synthetic approaches that enable precise control over size, morphology, and nanostructure.[7–12] A new class of metal–organic frameworks (MOFs), which are composed of an acidic ligand with DABCO, is called DMOFs as pillared MOFs.[13–16] Among MOFs, Zr-based metal–organic frameworks are applied as catalysts for the preparation of biologically active candidates such as pyrazolo[3, 4-b]pyridines, picolinates, (mono, bis, tris and tetrakis) pyrido[2,3-d]pyrimidines, dihydrobenzo[g]pyrimido[4,5-b]quinoline derivatives and dicyanomethylene pyridine derivatives.[17,18] Heterogeneous catalysts are essential in numerous chemical transformations, providing benefits like easy separation, reusability, and improved catalytic efficiency. Post-synthesis modifications further enhance their catalytic performance and broaden their functional diversity.[19–22] The structure–activity relationship is pivotal in utilizing metal–organic frameworks (MOFs) across diverse catalytic applications, including photocatalysis, electrocatalysis, material oxidation, biomass conversion, and acid-base catalysis. Very recently, the strategies to design and process MOFs for specific applications have been comprehensively reviewed.[23] The focal point of the mentioned review is the rationalization and identification of the design factors that lead to the production of optimal compositions, resultant performance parameters, structures and nanostructures.
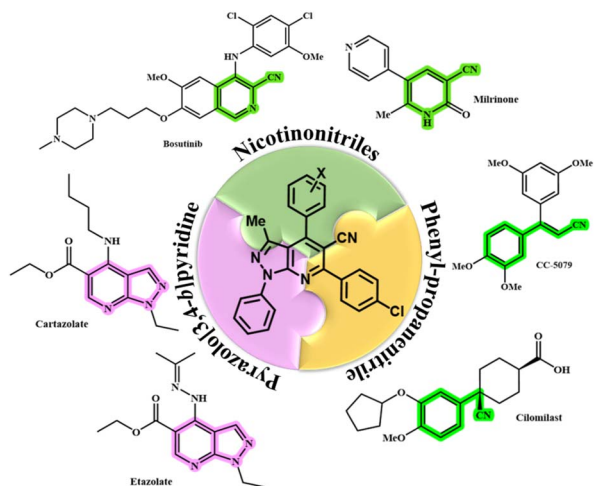
Biologically-inspired structures like pyridine as a *N*-heterocyclic building block in organic chemistry, commonly found in various pharmaceuticals, agrochemicals, and industrial chemicals.[24–26] The unique structure of pyridine imparts several interesting biological properties to this heterocyclic system (Scheme 1). Pyridine derivatives have been extensively studied for their pharmacological activities, including anti-inflammatory, anti-cancer, anti-bacterial, and anti-viral

[a]Department of Organic Chemistry, Faculty of Chemistry and Petroleum Sciences, Bu-Ali Sina University, PO Box 6517838683, Hamedan, Iran. E-mail: mhajjami@yahoo.com; mzolfigol@yahoo.com; Tel: +988138282807

[b]Department of Chemistry, Faculty of Science, University of Qom, Qom, 37185-359, Iran. E-mail: mahmoud8103@yahoo.com

[c]Department of Energy, Materials and Energy Research Centre, P.O. Box 31787-316, Karaj, 401602, Iran
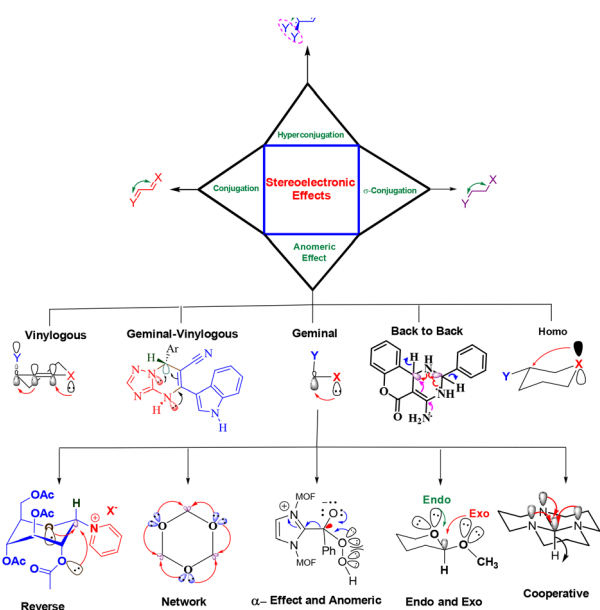
[d]School of Chemistry and Chemical Engineering, Huazhong University of Science and Technology, 1037 Luoyu Road, Hongshan District, Wuhan, 430074, China

Scheme 1 Structure of medicinal compounds containing nicotinonitrile, phenyl-propanenitrile and pyrazolo-pyridines.

properties.[27–32] The presence of the nitrogen atom in the pyridine ring allows for the formation of hydrogen bonds with biological targets, enhancing their binding affinity and biological activity.[33,34] Additionally, pyrazolo[3,4-*b*]pyridine rings have been shown to a broad spectrum of biological and pharmaceutical activities.[35,36] Consequently, addressing these challenges and limitations necessitates the creation of a novel and efficient reaction that offers high catalytic efficiency, reduced reaction times, and straightforward workup procedures for synthesizing pyrazolo[3,4-*b*]pyridines under neutral, mild, and practical conditions, which is of significant interest.

The concept of anomeric effects as a subset of the stereoelectronic effects introducing the electron sharing from donor to acceptor atoms.[37]

Scheme 2 Various kinds of stereoelectronic and anomeric effects.

Electrons are transferred from a lone pair of heteroatoms (X = N, O, *etc.*) to the anti-bonding orbital of the C–Y bond ($n_X \rightarrow \sigma^*_{C-Y}$), leading to various reported anomeric effects. Recently, we have comprehensively reviewed the crucial role of the anomeric effect in chemical processes, especially in organic reactions (Scheme 2).[38,39] The oxidation-reduction properties of sensitive biological compounds like NADPH and NADP$^+$ rely on the concept of the anomeric effect, highlighting its significance (Scheme 1s in SI). In recent years, our research group has explored the role of the anomeric effect in the *in situ* oxidation of organic compounds without the need for any oxidant.[40–42] Cooperative and vinylogous anomeric-based oxidation (CVABO) have been mini-reviewed.[43,44]

The presented work provides a comprehensive overview of the application of DMOF-Zr as a heterogeneous catalyst for thecatalytic preparation of a wide range of pyrazolo[3,4-*b*]pyridine derivatives. The attention of the current study will be focused on the structural features providing the best catalytic performance of DMOF-Zr and the mechanisms of their catalytic action.

Experimental

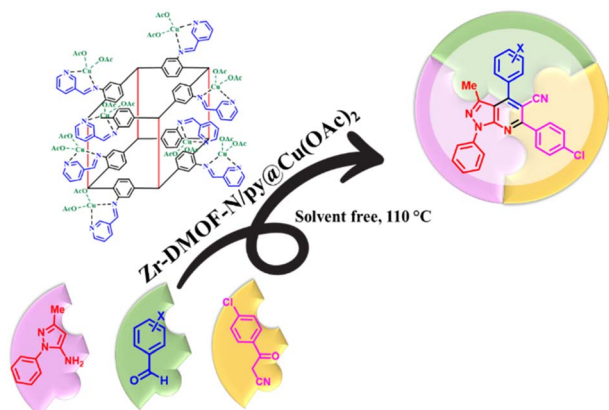### General procedure for the synthesis of Zr-DMOF-N/Py@Cu(OAc)$_2$

First, a solution was prepared by sonicating and dissolving ZrCl$_4$ (0.6 mmol, 0.14 g) in dry DMF (40 mL) referred to as solution 1. Concurrently, solution 2 was created by dissolving BDC-NH$_2$ (0.3 mmol, 0.054 g), and DABCO (0.3 mmol, 0.033 g) in dry DMF (20 mL). The two solutions were then combined and stirred with acetic acid (10 mL) at room temperature for 15 min. The resulting mixture was transferred into a Teflon-lined bomb (100 mL) and placed in an oven at 120 °C for 24 hours.[45,46]

After this period, the colloidal particles were isolated by centrifugation and washed with DMF and EtOH. Subsequently, a mixture of Zr-DMOF-NH$_2$ (0.5 g), nicotinaldehyde (2 mmol, 0.187 mL) and CH$_3$CN (50 mL) was added to another Teflon-lined bomb (100 mL) for 72 h.[47] The solid product was then separated by centrifuge, washed with ethanol, and dried in a vacuum oven at 60 °C for 12 h. In the final step, a mixture of Zr-DMOF-N/Py (0.5 g) and Cu(OAc)$_2$ (0.2 mmol, 0.036 g) was stirred in ethanol (20 mL) at room temperature for 2 h.[48] The particles were again separated by centrifugation and washed with EtOH (3 × 10 mL). Finally, the pure Zr-DMOF-N/Py@Cu(OAc)$_2$ was dried under vacuum at 80 °C, as illustrated in Scheme 4.
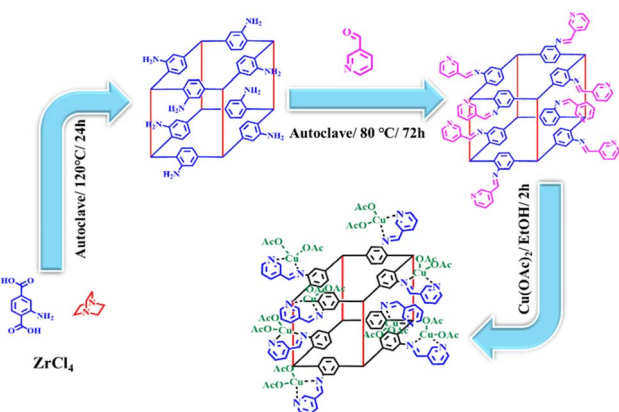
General procedure for the synthesis of pyrazolo[3,4-*b*]pyridines using Zr-DMOF-N/Py@Cu(OAc)$_2$ as a catalyst

In a 10 mL round-bottomed flask, a mixture consisting of aromatic aldehydes (1 mmol), 3-methyl-1-phenyl-1*H*-pyrazol-5-amine (1 mmol, 0.173 g), 3-(4-chlorophenyl)-3-oxopropanenitrile (1 mmol, 0.179 g), and Zr-DMOF-N/Py@Cu(OAc)$_2$ (20 mg) as catalyst were stirred at 110 °C under solvent free conditions. The reaction progress was monitored using TLC with a solvent system of *n*-hexane/ethyl acetate 6:4.

Scheme 3 Catalytic application of Zr-DMOF-N/Py@Cu(OAc)$_2$ for the preparation of pyrazolo[3,4-b]pyridine derivatives.

Scheme 4 Synthesis of Zr-DMOF-N/Py@Cu(OAc)$_2$ as a heterogeneous and porous catalyst.

Upon completion of the reaction, hot acetone was added to the mixture, and the catalyst was separated using centrifuged 1000 rpm (twice). The resulting solid precipitate was washed with EtOH to yield the desired pure pyrazolo[3,4-b]pyridine derivatives (see Scheme 3).

Results and discussions

The study presented involves the post-functionalization of target pillared layer mixed ligand metal–organic framework (DMOF-Zr) to synthesize a mesoporous catalyst, Zr-DMOF-N/Py@Cu(OAc)$_2$, which was characterized using various techniques. This catalyst was used for the synthesis of pyrazolo[3,4-b]pyridine derivatives. The stereochemistry and mechanism of these derivatives were also investigated. Some derivatives were noted in the study of the reaction mechanism to remain at the dihydropyran formation stage and not further on to the aromatization of the ring, while others continued to yield aromatic products and their corresponding pyridine rings. The aromatization and formation of the pyridine ring was established through a mechanism known as cooperative vinylogous anomeric-based oxidation. Anomeric concepts have recently been reviewed in the literature.[40–42,48]

The FT-IR spectrum analysis provides valuable information about the functional groups present in the catalysts Cu(OAc)$_2$, Zr-DMOF-NH$_2$, Zr-DMOF-N/Py, and Zr-DMOF-N/Py@Cu(OAc)$_2$. The two peaks at 3448 and 3364 cm^{-1} of NH$_2$ functional groups represent the synthesis of UiO-66-NH$_2$.[45] The clear presence of pyridine peaks in the final catalyst structure confirms the successful incorporation of this building block. The peak at 1626 cm^{-1} is related to the C=N double bond in Zr-DMOF-N/Py due to the reaction with Cu(OAc)$_2$ shifted to a higher frequency at about 1655 cm^{-1} in the catalyst. Also, the absorption peaks at 2856 and 2928 cm^{-1} are related to aromatic C–H and C=C stretch bands. Overall, the observed changes in the analyses of the catalysts throughout the synthesis steps suggest that the synthesis has proceeded as intended, leading to the formation of the desired catalyst structures (Fig. 1).
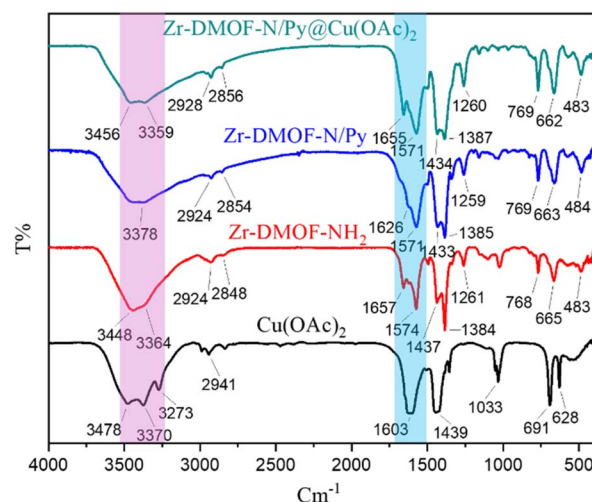

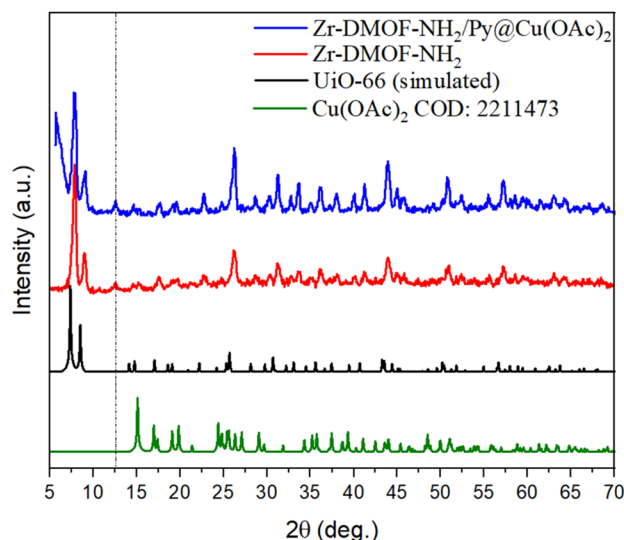**Fig. 1** FT-IR spectra of different stages of the synthesis of the catalyst.

Fig. 2 XRD pattern of different stages of the synthesis of the catalyst with UiO-66 (CCDC: 2054314) and Cu(OAc)$_2$ (COD:2211473).

© 2025 The Author(s). Published by the Royal Society of Chemistry

In another investigation, we conducted a comparison of the crystal patterns of Zr-DMOF-NH$_2$ and Zr-DMOF-N/Py@Cu(OAc)$_2$ using XRD analysis (Fig. 2). Initially, the original crystal structure was compared with the simulated UiO-66 structure,[49] and they appeared very similar. However, a peak at $2\theta = 12$ was observed, likely to indicate a slight structural change due to the presence of DABCO. Furthermore, the peak observed at $2\theta < 10$ suggests that the crystal plates of the various phases demonstrate adequate stability. This study confirms the successful synthesis of pillared layer mixed-ligand metal–organic framework functionalized with Cu(OAc)$_2$ while maintaining the integrity of the crystal structure.

The morphology of (a) Zr-DMOF-NH$_2$ and (b) Zr-DMOF-N/Py@Cu(OAc)$_2$ as a porous catalyst was studied by SEM technique (Fig. 3). According to Fig. 3, it can be concluded that Cu particle has been successfully added to the primary pillared layer mixed ligand metal–organic framework. Therefore, placing the Cu particle on Zr-UiO-66-NH$_2$ does not change its morphology, which indicates that the structure of the pillared layer mixed ligand metal–organic framework remains stable.

N$_2$-adsorption/desorption isotherms for both samples were measured and plotted in Fig. 4a. It is clear that the adsorbed N$_2$ decreased after modification of Zr-DMOF-NH$_2$ to Zr-DMOF-N/Py@Cu(OAc)$_2$. The calculated surface area based on BET equation and also total pore volume for Zr-DMOF-NH$_2$ are 760.35 m^2 g^{-1} and 0.65 cm^3 g^{-1} and for Zr-DMOF-N/Py@Cu(OAc)$_2$ are 501.13 m^2 g^{-1} and 0.466 cm^3 g^{-1}, respectively. Meanwhile, the pore size distribution of the samples calculated based on the BJH method is shown in Fig. 4b. These plots show that Zr-DMOF-NH$_2$ have both micropores and mesopores, but after modification the Zr-DMOF-N/Py@Cu(OAc)$_2$ sample has only
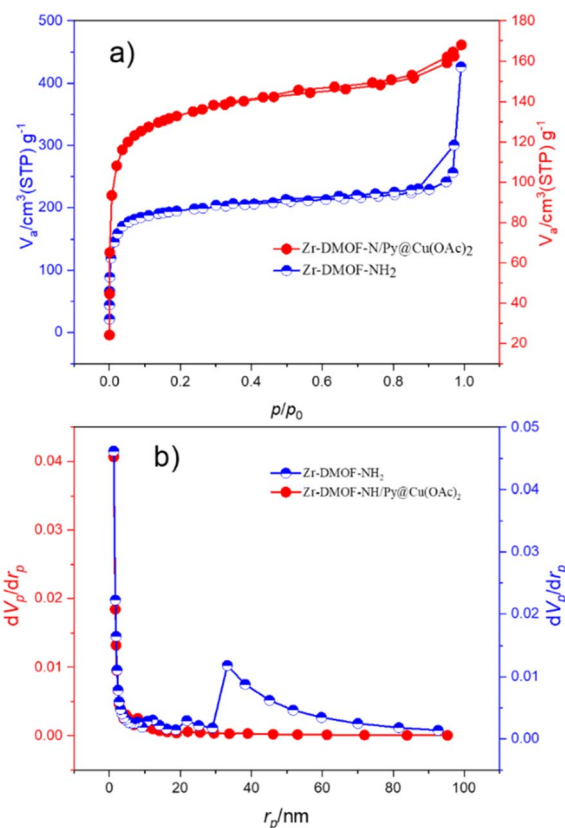

Fig. 4 (a) N$_2$ adsorption–desorption isotherms and (b) pore size distribution of Zr-DMOF-NH$_2$ and Zr-DMOF-N/Py@Cu(OAc)$_2$.

micropores. The average pore diameter for Zr-DMOF-NH$_2$ and Zr-DMOF-N/Py@Cu(OAc)$_2$ are 3.42 nm and 2.07 nm, respectively.
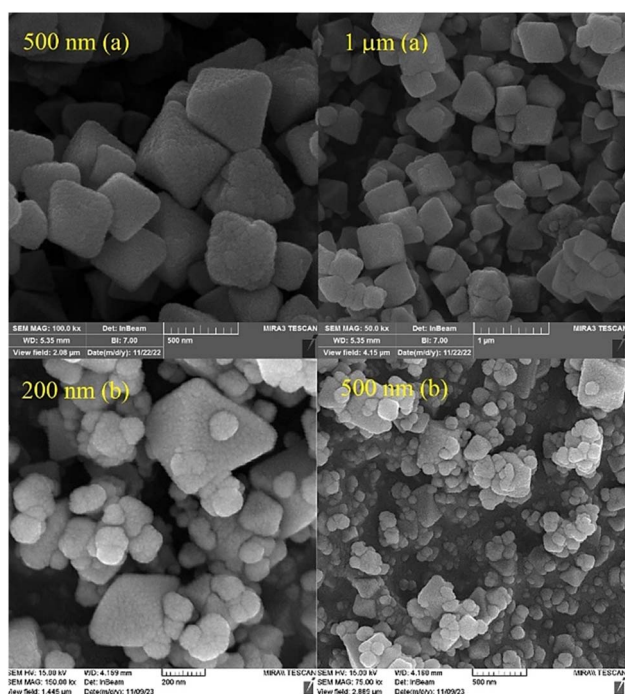

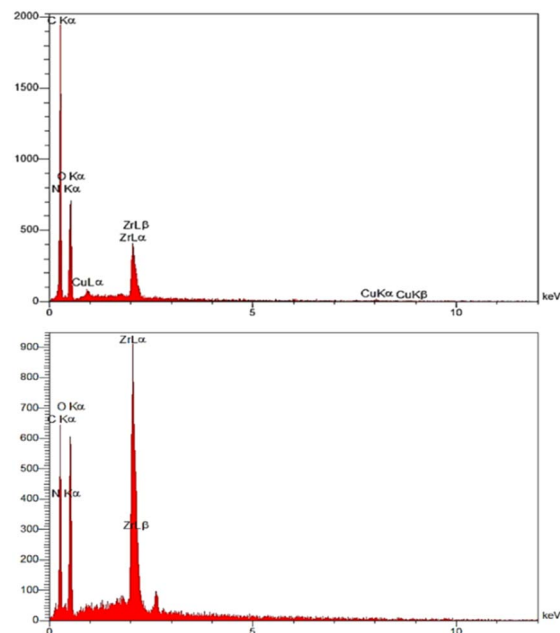Fig. 3 SEM image of (a) Zr-DMOF-NH$_2$ and (b) Zr-DMOF-N/Py@Cu(OAc)$_2$ as a porous catalyst.

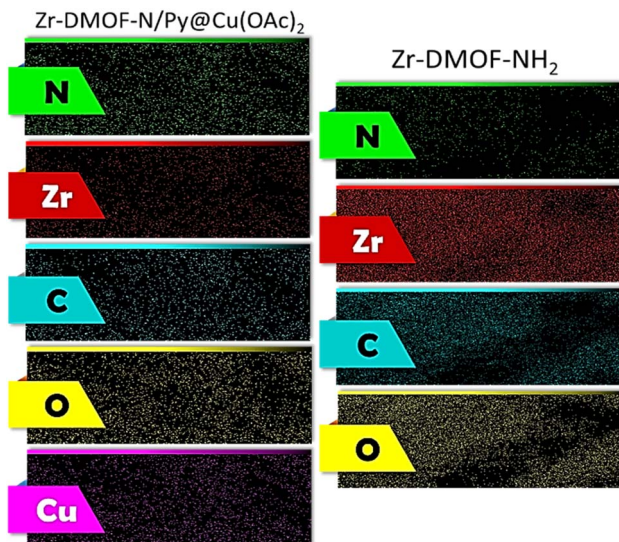Fig. 5 Energy-dispersive X-ray spectroscopy (EDX) for Zr-DMOF-NH$_2$ and Zr-DMOF-N/Py@Cu(OAc)$_2$.

Fig. 6 Elemental mapping analysis of Zr–DMOF–NH$_2$ and Zr–DMOF–N/Py@Cu(OAc)$_2$.

The atoms constituting the Zr–DMOF–NH$_2$ and Zr–DMOF–N/Py@Cu(OAc)$_2$ structure were identified using energy-dispersive X-ray spectroscopy (EDX) and elemental mapping analysis. The analysis confirmed the presence of carbon, nitrogen, copper, zirconium and oxygen in the functionalized metal–organic framework, as well as carbon, nitrogen, zirconium and oxygen atoms in the base metal–organic framework structure (Fig. 5).

Additionally, elemental mapping demonstrated and validated the uniform distribution of elements within the Zr–DMOF–NH$_2$ and Zr–DMOF–N/Py@Cu(OAc)$_2$ structures (Fig. 6).

In another analysis, the stability of Zr–DMOF–N/Py@Cu(OAc)$_2$ was evaluated using thermogravimetric analysis (TGA) analysis (see Fig. 7). The first weight loss occurs below 100 °C, which is associated with the release of organic solvents used during the catalyst synthesis. The second weight loss at approximately 300 °C likely corresponds to the detachment

Cu(OAc)$_2$ from the catalyst's surface. The third weight loss observed around 400 °C is probably linked to the removal of imidazole from the catalyst structure. Based on these results, the designed catalyst demonstrated good catalytic properties and can be utilized effectively at temperatures up to 300 °C.

After the synthesis and characterization of Zr–DMOF–N/Py@Cu(OAc)$_2$ as a catalyst, it was used for the synthesis of pyrazolo[3,4-b]pyridine derivatives. The catalytic performance of Zr–DMOF–N/Py@Cu(OAc)$_2$ was well determined based on the results obtained. The reaction involving 3-methyl-1-phenyl-1H-pyrazol-5-amine (1 mmol, 0.173 g), 4-chlorobenzaldehyde (1.0 mmol, 0.141 g) and 3-(4-chlorophenyl)-3-oxopropanenitrile (1 mmol, 0.179 g) were tested as a model reaction. The model reaction was evaluated at different amounts of catalyst and temperatures (Table 1, entries 1–11). Also, the model reaction was investigated using various solvents such as n-hexane, EtOAc, EtOH, H$_2$O, MeOH, CH$_3$CN, EtOH: H$_2$O (5 mL) and solvent-free were used in the presence of 20 mg of Zr–DMOF–N/Py@Cu(OAc)$_2$ under reflux conditions (Table 1, entries 12–18). However, the results of the reaction did not show any improvement. The optimal reaction conditions for the synthesis of 4,6-bis(4-chlorophenyl)-3-methyl-1-phenyl-1H-pyrazolo[3,4-b]pyridine was achieved using Zr–DMOF–N/Py@Cu(OAc)$_2$ (20 mg) under solvent-free conditions at 110 °C (Table 1, entry 2).

Following the optimization of the reaction conditions, the efficiency and applicability of Zr–DMOF–N/Py@Cu(OAc)$_2$ were evaluated through the reaction of 3-methyl-1-phenyl-1H-pyrazol-5-amine (1 mmol), 3-(4-chlorophenyl)-3-oxopropanenitrile (1 mmol) and various aromatic aldehyde

Table 1 Optimization of some reaction's parameters for the synthesis of pyrazolo[3,4-b]pyridine using Zr–DMOF–N/Py@Cu(OAc)$_2$
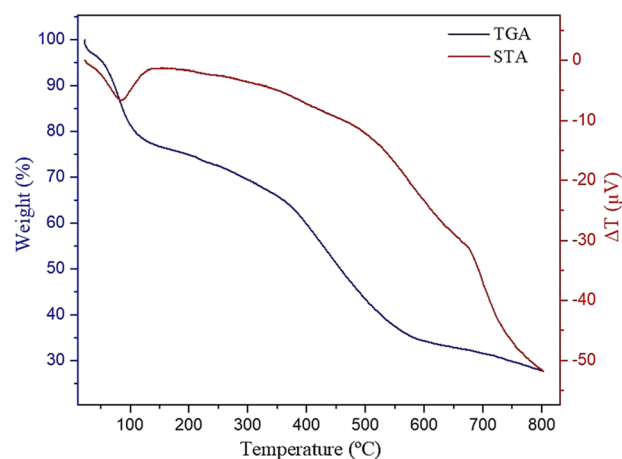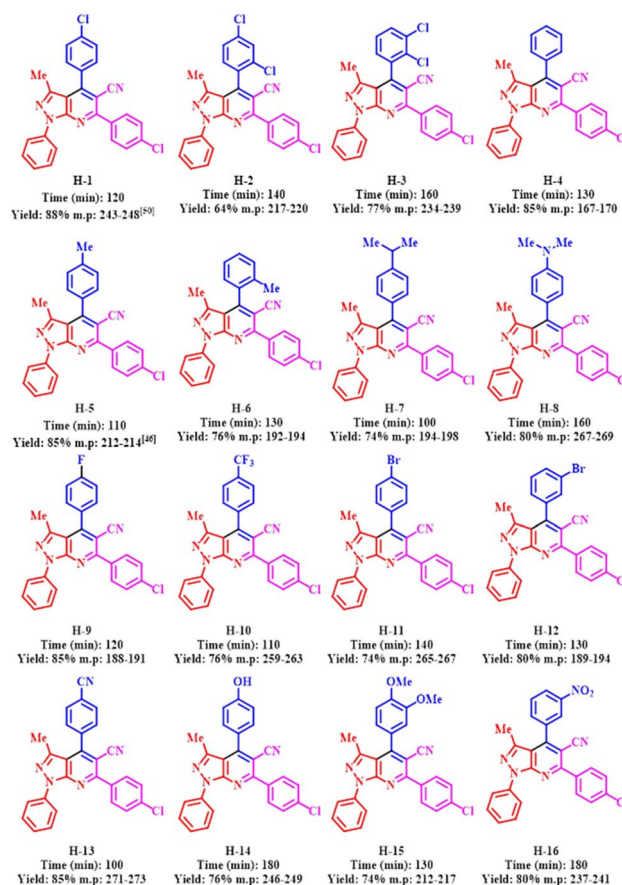

Entry	Cat. (mg)	Temp. (°C)	Solvent	Time (h)	Yield (%)
1	25	110	—	2	82
2	**20**	**110**	**—**	**2**	**88**
3	15	110	—	2	76
4	10	110	—	2	55
5	5	110	—	2	42
6	—	110	—	2	Trace
7	20	r.t.	—	2	Trace
8	20	50	—	2	40
9	20	70	—	2	60
10	20	90	—	2	65
11	20	120	—	2	88
12	20	Reflux	n-Hexane	6	0
13	20	Reflux	EtOAc	6	0
14	20	Reflux	EtOH	8	55
15	20	Reflux	H$_2$O	6	0
16	20	Reflux	MeOH	8	63
17	20	Reflux	CH$_3$CN	8	55
18	20	Reflux	EtOH: H$_2$O	7	30

Fig. 7 TG/STA analysis of Zr–DMOF–N/Py@Cu(OAc)$_2$.

Paper

Table 2 Synthesis of pyrazolo[3,4-b]pyridine derivatives using Zr–DMOF–N/Py@Cu(OAc)$_2$ [50]

both electron-withdrawing and electron-releasing using Zr-DMOF-N/Py@Cu(OAc)$_2$ (20 mg) as a catalyst at 110 °C under the solvent-free condition. The results obtained are summarized in Table 2.

As indicated in Table 2, all synthesized derivatives were produced under environmentally friendly and mild conditions,

demonstrating the effective catalytic performance of Zr-DMOF-N/Py@Cu(OAc)$_2$. A wide range of aldehydes, including various aromatic aldehydes with electron-donating, electron-withdrawing and halogens substituents, yielded the desired pyrazolo[3,4-b]pyridine derivatives in high to excellent yields

Table 3 Comparison of the various catalysts in the synthesis of pyrazolo[3,4-b]pyridine derivatives

Entry	Catalyst	Amount of catalysts (mg)	Time (min)	Yield (%)
1	SSA	20	180	40
2	CQDs-N(CH$_2$PO$_3$H$_2$)$_2$/SBA-15 (ref. 51)	20	120	42
3	N(Et)$_3$	20 mol%	180	70
4	p-TSA	20 mol%	180	57
5	[Zr-UiO-66-CO$_2$H]Br (ref. 52)	20	120	61
6	Fe$_3$O$_4$@SiO$_2$@tosyl-carboxamide (ref. 42)	20	120	75
7	MIL-88B(Fe$_2$/Co)-N(CH$_2$PO$_3$H$_2$)$_2$ (ref. 53)	20	120	50
8	Cu(OAc)$_2$	20 mol%	120	80
9	Zr-DMOF-NH$_2$	20	120	52
10	Zr-DMOF-NH$_2$/Py	20	120	63
11	**Zr-DMOF-NH$_2$/Py@Cu(OAc)$_2$**	**20**	**120**	**88**
12	MIL-88B(Fe$_2$/Co)-Bnta-[CH$_2$CO$_2$H]Br (ref. 25)	20	120	66
13	Poly(acetic acid)	20	180	51
14	Pipyridine	20 mol%	180	72
15	KOH	20 mol%	180	57
16	ZrCl$_4$	20 mol%	210	62

(88%) within relatively short reaction times (120 min.) (see Table 2).

In order to evaluate the efficiency of Zr-DMOF-N/Py@Cu(OAc)$_2$ as a pillared layer mixed ligand metal–organic framework based on Zr-catalyst, various organic and inorganic catalysts as well as Zr-DMOF-N/Py@Cu(OAc)$_2$ were studied in the reaction of 3-methyl-1-phenyl-1H-pyrazol-5-amine (1 mmol, 0.173 g), 4-chlorobenzaldehyde (1.0 mmol, 0.141 g) and 3-oxo-3-phenylpropanenitrile (1 mmol, 0.179 g). The results obtained are shown in Table 3.

In the suggested mechanism, Zr-DMOF-N/Py@Cu(OAc)$_2$ activates the carbonyl part of aldehyde structure. Also, 3-oxo-3-phenylpropanenitrile converts to the enol form with the assistance of Zr-DMOF-N/Py@Cu(OAc)$_2$. Next, during the attack of the enol form of 3-oxo-3-phenylpropanenitrile to the activated aldehyde *via* Knoevenagel condensation is formed intermediate (I). In the next step, intermediate (I) reacts with 3-methyl-1-phenyl-1H-pyrazol-5-amine as a Michael acceptor to produce intermediate (II). Intermediate (III) is formed from cyclization and tautomerization intermediate (II). Subsequently, intermediate (III) is converted to 1,4-dihydropyridines as intermediate (IV) by the elimination of one molecule of H$_2$O. Finally, intermediate (IV) forms a pyridine structure *via* a CVABO mechanism, which leads to the release of one hydrogen molecule (–H$_2$) and/or hydrogen peroxide (–H$_2$O$_2$)[40–42,48] (Scheme 5).

The utilization of Zr-DMOF-N/Py@Cu(OAc)$_2$ as a pillared layer mixed ligand metal–organic framework based on Zr-
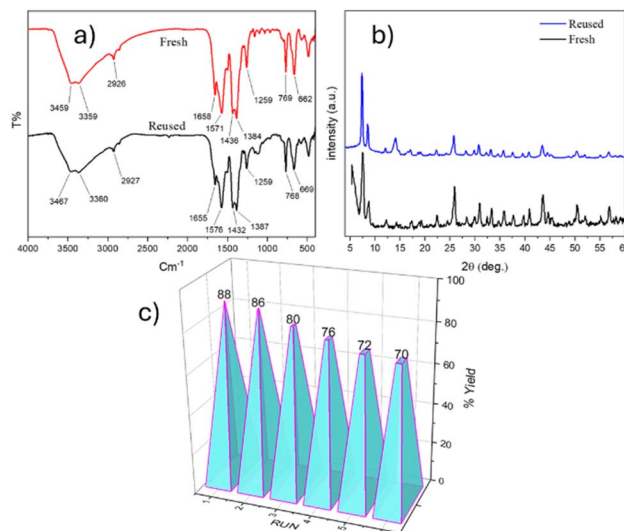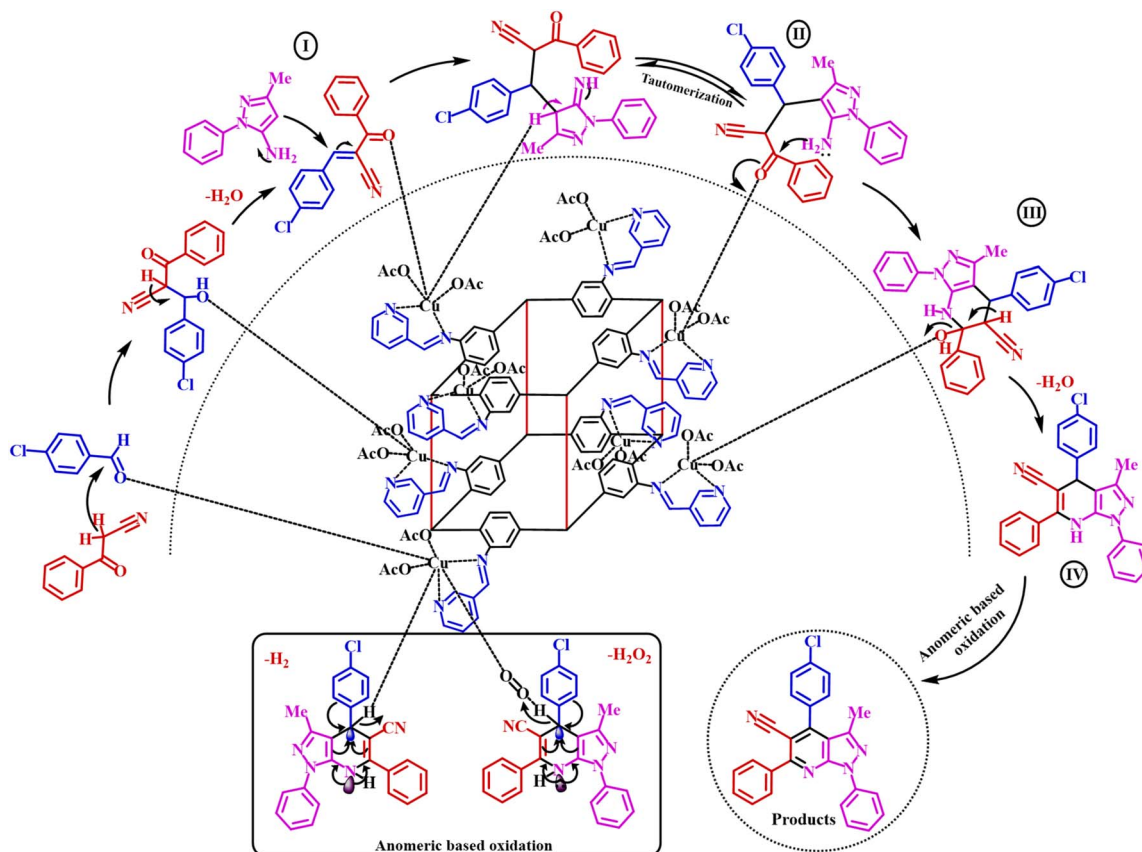

Fig. 8 (a) FT-IR and (b) XRD analysis of fresh and reused Zr–DMOF-N/Py@Cu(OAc)$_2$. (c) Recyclability of Zr-DMOF-N/Py@Cu(OAc)$_2$ as catalyst in the synthesis of pyrazolo[3,4-b]pyridine derivatives.

catalyst shows the best results in terms of efficiency for the synthesis of pyrazolo[3,4-b]pyridine derivatives. Additionally, the recyclability of the catalyst was also investigated in the model reaction, demonstrating that the catalyst can be recycled and reused 5 times without significant change in efficiency. To

Scheme 5 Suggested mechanism for the synthesis of pyrazolo[3,4-b]pyridine derivatives.

conduct further examination, the recycled catalyst underwent FT-IR and XRD analysis. The FT-IR analysis indicated that the peaks remained unchanged, but there was a slight broadening in the 2600 to 3500 cm^{-1} regions due to impurities and hydrogen bond formation. Additionally, the XRD analysis revealed that the spectra of the recycled and fresh catalysts were entirely similar, suggesting that the crystal planes and structure remained stable. To further explore this, a leaching test was conducted to examine the chemical stability of the catalyst. To do this, the model reaction was carried out using the catalyst of interest, and then the catalyst was separated from the reaction mixture for ICP-OES analysis. The findings revealed that 5 ppm Zr and 11.6 ppm Cu from Zr-DMOF-N/Py@Cu(OAc)$_2$ was detected. According to the results, Zr-DMOF-N/Py@Cu(OAc)$_2$ is the best catalyst for the synthesis of pyrazolo[3,4-b]pyridine derivatives (Fig. 8).

Conclusions

In this study, we designed and synthesized a pillared layer mixed ligand metal–organic framework using zirconium (Zr) as a metal component. The resulting framework, termed DMOF-Zr was synthesized with Cu(OAc)$_2$ through a post-modification approach. The incorporation of both Zr metals and Cu(OAc)$_2$ within the catalyst structure enhances its catalytic activity. The synthesized Zr-DMOF-N/Py@Cu(OAc)$_2$ was well characterized by various analytical techniques. This catalyst was evaluated for its effectiveness in synthesizing pyrazolo[3,4-b]pyridine derivatives, which are promising candidates for biological and pharmaceutical applications, *via* a cooperative vinylogous anomeric-based oxidation process. Key advantages of this research include the synthesis in mild and green conditions, recycling and reusability of catalyst and high yield of desired products.

Author contributions

H. A.: methodology, validation, investigation. M. A. Z.: supervision, resources, project administration, funding acquisition, conceptualization, writing – review. M. Z.: investigation and writing the original draft. M. H.: supervision. M. H.: catalyst characterization. Y. G.: materials.

Conflicts of interest

The authors declare no conflict of interest.

Data availability

The datasets used and/or analyzed during the present study are available from the corresponding author upon reasonable request. All data generated or analyzed during this study are included in this published article [and its SI file].

Supplementary information: instrument, materials, FT-IR, ^{1}H NMR and ^{13}C NMR spectra for the pyrazolo[3,4-b]pyridine derivatives. See DOI: **https://doi.org/10.1039/d5ra03078a**.

Acknowledgements

References

1 Y. S. Wei, M. Zhang, R. Zou and Q. Xu, *Chem. Rev.*, 2020, **120**, 12089–12174.

2 X. Zhang, Z. Chen, X. Liu, S. L. Hanna, X. Wang, R. Taheri-Ledari and O. K. Farha, *Chem. Soc. Rev.*, 2020, **49**, 7406–7427.

3 M. Y. Masoomi, A. Morsali, A. Dhakshinamoorthy and H. Garcia, *Angew. Chem.*, 2019, **131**, 15330–15347.

4 D. Zhu, Y. Chen, Y. Zhu, C. Y. Liu, Q. Yan, X. Wu and R. Verduzco, *Macromolecules*, 2024, **57**, 1038–1049.

5 H. Liu, C. Li, H. Li, Y. Ren, J. Chen, J. Tang and Q. Yang, *ACS Appl. Mater. Interfaces*, 2020, **12**, 20354–20365.

6 J. Tang and Y. Yamauchi, *Nat. Chem.*, 2016, **8**, 638–639.

7 S. Mandal, S. Natarajan, P. Mani and A. Pankajakshan, *Adv. Funct. Mater.*, 2021, **31**, 2006291.

8 S. Mallakpour, E. Nikkhoo and C. M. Hussain, *Coord. Chem. Rev.*, 2022, **451**, 214262.

9 Y. Qian, F. Zhang and H. Pang, *Adv. Funct. Mater.*, 2021, **31**, 2104231.

10 K. Yue, X. Zhang, S. Jiang, J. Chen, Y. Yang, F. Bi and Y. Wang, *J. Mol. Liq.*, 2021, **335**, 116108.

11 J. Hwang, A. Ejsmont, R. Freund, J. Goscianska, B. V. Schmidt and S. Wuttke, *Chem. Soc. Rev.*, 2020, **49**, 3348–3422.

12 H. Sepehrmansourie, H. Alamgholiloo, N. N. Pesyan and M. A. Zolfigol, *Appl. Catal., B*, 2023, **321**, 122082.

13 Y. Hong, Y. Wang, Y. Guo, K. Wang, H. Wu, C. Zhang, Q. Zhang and Z. fur, *Anorg. Allg. Chem.*, 2022, **648**, e202200115.

14 H. Liu, W. Ye, Y. Mu, H. Ma, A. Lv, S. Han and W. Huang, *Adv. Mater.*, 2022, **34**, 2107612.

15 E. Tavakoli, H. Sepehrmansourie, M. Zarei, M. A. Zolfigol, A. Khazaei, A. Mohammadzadeh and E. Ghytasranjbar, *J. Mater. Chem. C*, 2024, **12**, 9392–9400.

16 I. Senkovska, V. Bon, L. Abylgazina, M. Mendt, J. Berger, G. Kieslich and S. Kaskel, *Angew. Chem.*, 2023, **135**, e202218076.

17 F. Jalili, M. Zarei, M. A. Zolfigol and A. Khazaei, *RSC Adv.*, 2022, **12**, 9058–9068.

18 H. Ahmadi, M. Zarei and M. A. Zolfigol, *ChemistrySelect*, 2022, **7**, e202202155.

19 T. A. Goetjen, J. Liu, Y. Wu, J. Sui, X. Zhang, J. T. Hupp and O. K. Farha, *Chem. Comm.*, 2020, **56**, 10409–10418.

20 A. Radwan, H. Jin, D. He and S. Mu, *Nano-Micro Lett.*, 2021, **13**, 1–32.

21 H. Sepehrmansourie, H. Alamgholiloo, M. A. Zolfigol, N. N. Pesyan and M. M. Rasooll, *ACS Sustain. Chem. Eng.*, 2023, **11**, 3182–3193.

22 J. C. Wang, F. W. Ding, J. P. Ma, Q. K. Liu, J. Y. Cheng and Y. B. Dong, *Inorg. Chem.*, 2015, **54**, 10865–10872.

23 T. De Villenoisy, X. Zheng, V. Wong, S. S. Mofarah, H. Arandiyan, Y. Yamauchi, P. Koshy and C. C. Sorrell, *Adv. Mater.*, 2023, **35**, 2210166.

24 G. Mohammad Abu-Taweel, M. M. Ibrahim, S. Khan, H. M. Al-Saidi, M. Alshamrani, F. A. Alhumaydhi and S. Alharthi, *Crit. Rev. Anal.*, 2024, **54**, 599–616.

25 S. A Patil, A. P Hoagland, S. A Patil and A. Bugarin, *Future Med. Chem.*, 2020, **12**, 2239–2275.

26 A. Y. Guan, C. L. Liu, X. F. Sun, Y. Xie and M. A. Wang, *Med. Chem.*, 2016, **24**, 342–353.

27 R. Sahu, R. Mishra, R. Kumar, C. Majee, A. Mazumder and A. Kumar, *Mini Rev. Med. Chem.*, 2022, **22**, 248–272.

28 P. Singh, *Recent Developments in the Synthesis and Applications of Pyridines*, Elsevier, 2022.

29 R. Abbas and P. H. Hsyu, *Pharmacokinet.*, 2016, **55**, 1191–1204.

30 L. Y. Z. Chong, K. Satya, B. Kim and R. Berkowitz, *Cardiol. Rev.*, 2018, **26**, 35–42.

31 C. Kroegel and M. Foerster, *Expert. Opin. Investig. Drugs*, 2007, **16**, 109–124.

32 H. N. Vu, W. J. Miller, S. A. O'Connor, M. He, P. H. Schafer, F. Payvandi and S. K. Libutti, *J. Surg. Res.*, 2010, **164**, 116–125.

33 E. Kutlu, F. M. Emen, G. Kismali, N. K. Kınaytürk, D. Kılıç, A. I. Karacolak and R. E. Demirdogen, *J. Mol. Struct.*, 2021, **1234**, 130191.

34 P. W. Kenny, *J. Med. Chem.*, 2022, **65**, 14261–14275.

35 R. F. Barghash, W. M. Eldehna, M. Kovalova, V. Vojáčková, V. Kryštof and H. A. Abdel-Aziz, *Eur. J. Med. Chem.*, 2022, **227**, 113952.

36 A. A. Farahat, E. M. Samir, M. Y. Zaki, R. A. Serya and H. A. Abdel-Aziz, *Arch. Pharm.*, 2022, **355**, 2100302.

37 I. V. Alabugin, L. Kuhn, N. V. Krivoshchapov, P. Mehaffy and M. G. Medvedev, *Chem. Soc. Rev.*, 2021, **50**, 10212–10252.

38 I. V. Alabugin, L. Kuhn, M. G. Medvedev, N. V. Krivoshchapov, V. A. Vil, I. A. Yaremenko and M. A. Zolfigol, *Chem. Soc. Rev.*, 2021, **50**, 10253–10345.

39 E. Matamoros, E. M. Pérez, M. E. Light, P. Cintas, R. F. Martínez and J. C. Palacios, *J. Org. Chem.*, 2024, **89**, 7877–7898.

40 S. Kalhor, M. Zarei, M. A. Zolfigol, H. Sepehrmansourie, D. Nematollahi, S. Alizadeh and J. Arjomandi, *Sci. Rep.*, 2021, **11**, 19370.

41 F. Jalili, H. Sepehrmansourie, M. Zarei, M. A. Zolfigol, A. Khazaei and M. A. As' Habi, *Arab. J. Chem.*, 2024, **17**, 105635.

42 M. Navazeni, M. A. Zolfigol, H. Ahmadi, H. Sepehrmansourie, A. Khazaei and M. Hosseinifard, Design, *RSC Adv.*, 2024, **14**, 16607–16616.

43 M. Yarie, *Iran. J. Catal.*, 2017, **7**, 85–88.

44 M. Yarie, *Iran. J. Catal.*, 2020, **10**, 79–83.

45 M. A. Zolfigol, S. Azizian, M. Torabi, M. Yarie and B. Notash, *J. Chem. Edu.*, 2024, **101**, 877–881.

46 J. Hungerford, S. Bhattacharyya, U. Tumuluri, S. Nair, Z. Wu and K. S. Walton, *J. Phys. Chem. C*, 2018, **122**, 23493–23500.

47 T. Gadzikwa and P. Matseketsa, *Dalton Trans.*, 2024, **53**, 7659–7668.

48 E. Tavakoli, H. Sepehrmansourie, M. Zarei, M. A. Zolfigol, A. Khazaei and M. A. As' Habi, *Sci. Rep.*, 2023, **13**, 9388.

49 (*a*) Y. Ma, X. Han, S. Xu, Z. Wang, W. Li, I. Da Silva, C. Sarayute, D. Lee, Y. Zou, M. Nikiel, P. Manuel, A. M. Sheveleva, F. Tuna, E. J. L. McInnes, Y. Cheng, S. Rudić, A. J. Ramirez-Cuesta, S. J. Haigh, C. Hardacre, M. Schröder and S. Yang, *J. Am. Chem. Soc.*, 2021, **143**, 10977–10985; (*b*) X. Y. Wang, X. T. Deng and C. G. Wang, *Struct. Rep.*, 2006, **62**, 3578–3579.

50 Z. Huang, Y. Hu, Y. Zhou and D. Shi, *ACS Comb. Sci.*, 2011, **13**, 45–49.

51 M. M. Rasooll, H. Sepehrmansourie, M. Zarei, M. A. Zolfigol and S. Rostamnia, *Sci. Rep.*, 2022, **12**, 20812.

52 A. R. Ataee-Najari, M. Zarei, H. Ahmadi, M. A. Zolfigol, A. Ghorbani-Choghamarani and M. Hosseinifard, *Polycycl. Aromat. Compd.*, 2024, **44**, 3442–3455.

53 M. M. Rasooll, H. Sepehrmansourie, M. Zarei, M. A. Zolfigol, M. Hosseinifard and Y. Gu, *ACS omega*, 2023, **8**, 25303.